Determination of the location and order of the drying transition with a molecular-dynamics simulation

M. J. P. Nijmeijer, C. Bruin, and A. F. Bakker
Laboratorium voor Technische Natuurkunde, P.O. Box 5046, 2600 GA Delft, The Netherlands

J. M. J. van Leeuwen
Instituut Lorentz, P.O. Box 9506, 2300 RA Leiden, The Netherlands
(Received 21 March 1991; revised manuscript received 23 May 1991)

The wetting transition is mostly found to be first order, but the nature of the drying transition in realistic systems is debated. We have simulated the wetting and drying of a wall and, by a careful inspection of the variation of the contact angle on the approach of the transition, find strong evidence for a continuous drying transition. Moreover, the drying point is located an order of magnitude more accurately with respect to previous attempts.

Wetting and drying phase transitions have drawn a substantial interest in the past decade[1] not only for their importance in technical applications but also as demonstrations of genuine surface phase transitions. After their discovery by Cahn[2] and by Ebner and Saam[3] on theoretical grounds and the experimental demonstration by Moldover and Cahn,[4] most of the theoretical studies have taken place in the context of lattice models,[5] on a mesoscopic level as variants of Landau's mean-field theory[1,6] or in the framework of density-functional theories.[7–9] None of these theories is capable of making an accurate prediction for the nature of the wetting and drying transitions for realistic systems. The lattice-gas models involve interactions which are too much simplified to describe the delicate balance between the driving forces in the wetting or drying of a real substrate. In its simplest form, the basic symmetry between particles and holes makes wetting and drying two mirror images of the same physical mechanism. The Landau-type mean-field theories help to classify the possible scenarios for wetting and drying but cannot make contact with a microscopic Hamiltonian. Density-functional theory should in principle be able to yield information on the phase diagram of realistic systems and some impressive results have indeed been obtained, e.g., by Velasco and Tarazona.[8] The strength and weakness of the density-functional theory have recently been reviewed by van Swol and Henderson.[7]

In this situation, computer simulations[9,10,12–14] are most welcome but so far rare because a large system is needed to accommodate the various phases involved and large fluctuations occur near the phase transitions, which slow down the approach to equilibrium. The results of simulations and density-functional calculations, tailored to the simulated systems, can be compared directly. Both yield in general a first-order wetting transition and agree on the location of the wetting point. The situation about the drying point is less clear. The simulations[9,10] of Henderson and co-workers indicate a first-order drying transition for both square-well and truncated Lennard-Jones systems. They consider[10] a smooth interpolation of the fluid's structure between a substrate-liquid and substrate-vapor interface, characteristic for a continuous transition, unlikely. Nevertheless, their density-functional calculation predicts a continuous (second-order) drying transition that is also located rather far from the simulation result. They attribute the first-order nature of the transition to large-scale fluctuations which are naturally present in the simulations but are not treated accurately by the density-functional theory. Velasco and Tarazona carried out a density-functional calculation on a Lennard-Jones system and initially found the drying transition to be weakly first order.[8] An improved calculation however showed second-order drying.[11] Their location of the drying transition was inconsistent with the results of the simulation[2] of Sikkenk *et al.* but this discrepancy has been removed by improved simulations,[13,14] which, however, could not decide on the order, being consistent with a continuous as well as a weakly first-order transition. In this Brief Report, we describe a simulation experiment that improves the accuracy by an order of magnitude, thereby clarifying the simulation results on the drying point.

The simulated system[12,14] consists of a three-dimensional cubic box with periodic boundary conditions in which a substrate is constructed by three layers of a fcc lattice of substrate particles. The remaining volume is occupied by a Lennard-Jones fluid consisting of a liquid and a vapor phase at a fixed temperature. By the boundary conditions, the fluid can wet or dry both sides of the substrate wall (see Fig. 1). The Lennard-Jones interactions ϕ_{AB} between particles of type A and B, where A and B stand for s in case of a solid and f in case of a fluid particle, are characterized by an energy scale ε_{AB} and a length scale σ_{AB}. They are truncated at $2.5\sigma_{AB}$ and shifted such as to remove the discontinuity at the truncation point. The reduced temperature T^*, defined as $T^*=k_BT/\varepsilon_{ff}$ is kept at 0.9 and the system contains 8400 fluid particles in a box with a linear dimension L of $29.1\sigma_{ff}$. We are able to simulate such large systems for

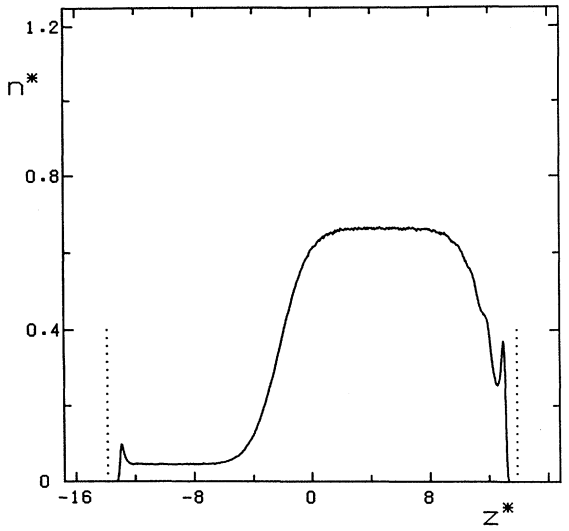

FIG. 1. The fluid's density n averaged over the x-y plane as a function of the position z between the outer layers of the wall. The density and position are expressed in reduced units: n^* equals n/σ_{ff}^3 and z^* denotes z/σ_{ff}. The dotted lines give the positions of the outer wall layers. The profile is calculated as an average over 5200 particle configurations, obtained in a run of 67 000 time steps at $\varepsilon_{sf}=0.25\varepsilon_{ff}$.

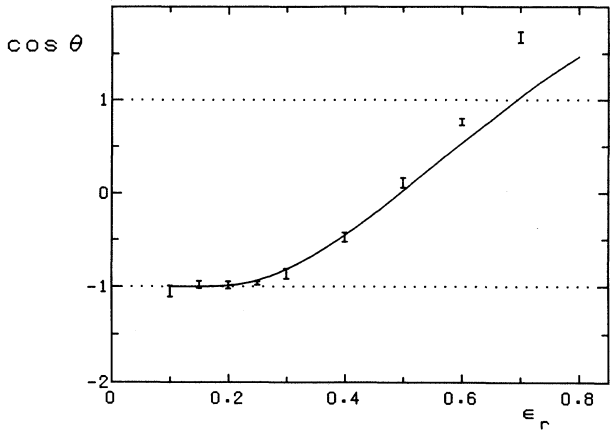

FIG. 2. $\cos\theta$ as a function of ε_r. The bars denote the measured $\cos\theta$, the curve is obtained by integrating the $\partial\cos\theta/\partial\varepsilon_{sf}$ data (see Fig. 3). The lengths of the bars denote the uncertainty in the measurement. They are calculated as the standard deviation in subaverages over 5200 time steps each. The data points comprise 5–25 subaverages.

long simulation runs because of the availability of a special purpose computer: the Delft Molecular-Dynamics Processor (DMDP).[15] The phase transitions are driven by varying the strength ε_{sf} of the interaction between wall and fluid particles. Our setup is particularly suited to study the partially wet (or dry) situation where $\varepsilon_d<\varepsilon_{sf}<\varepsilon_w$ with ε_d and ε_w the values of ε_{sf} where the drying and the wetting transition take place. In this situation of partial wetting and drying, the free energy favors one of the substrate sides to be covered by the liquid phase and the other by the vapor phase. Thus we have simultaneously realized a substrate-liquid, a substrate-vapor, and a liquid-vapor interface and we can obtain their surface tensions γ_{sl}, γ_{sv}, and γ_{lv} as integrals over pressure tensor components.[13] This situation is analogous to a liquid droplet adsorbed at a substrate making a contact angle θ with the substrate. The simulation data are thus interpreted in terms of a contact angle through Young's relation[1]

$$\cos\theta=\frac{\gamma_{sv}-\gamma_{sl}}{\gamma_{lv}} . \tag{1}$$

It turns out[13,14] that the difference $(\gamma_{sv}-\gamma_{sl})$ is obtained most accurately when the wall particles are frozen in at their lattice positions. So we use an inert wall representation, where the wall can be viewed as an external potential $\phi^{\rm ext}$ acting on the fluid. The results for $\cos\theta$ as a function of the ratio $\varepsilon_r=\varepsilon_{sf}/\varepsilon_{ff}$ are shown in Fig. 2. The drying transition, i.e., the point ε_d where $\cos\theta=-1$, is difficult to locate while the wetting point ε_w is fairly accurately given by the $\cos\theta$ data. The reason is that $\cos\theta$ cuts the line $\cos\theta=1$ at a steep angle while it joins the line $\cos\theta=-1$ much more smoothly. This is related to the nature of the phase transitions: $\cos\theta$ being essentially a free energy, the behavior of its derivative with respect to ε_{sf} gives the order of the phase transition. On the basis of these $\cos\theta$ measurements, the wetting and drying transitions were estimated[14] at $\varepsilon_w=0.62\pm0.01$ and $\varepsilon_d=0.20\pm0.05$, respectively (with ε_w and ε_d expressed in units of ε_{ff}).

The key to a more accurate analysis is a direct evaluation of the derivative $\partial\gamma_{sf}/\partial\varepsilon_{sf}$. For an inert wall, the derivative is given by the simple expression

$$\frac{\partial\gamma_{sf}}{\partial\varepsilon_{sf}}=\frac{1}{L^2}\int_{-L/2}^{L/2}dx\,dy\int_0^{z_c}dz\,n(\mathbf{r})\frac{\phi^{\rm ext}(\mathbf{r})}{\varepsilon_{sf}} . \tag{2}$$

Here, $n(\mathbf{r})$ is the fluid density, L the box size and z_c the cutoff in the substrate-fluid interaction, which is in our case $2.5\sigma_{sf}$ away from the outer layers of the wall. An accurate determination of the fluid density inside the potential of the substrate suffices to evaluate the derivative of γ_{sf}. The derivative of $\cos\theta$ is obtained from Young's law. Equation (2) follows from a direct differentiation of the partition function.[7]

As already indicated in Fig. 2, we simulated a series of partially wet (or dry) systems over a range of ε_r varying from 0.1 to 0.8. Typical runs involve 16 000 time steps for equilibration and some 100 000 time steps during which the system is sampled for accurate statistics. The longest simulation runs occurred around the drying transition where the fluctuations turned out to be large. Error bars in the data denote the standard deviation as calculated from subaverages over 400 configurations.

For $\varepsilon_{sf}<\varepsilon_d$, the liquid slab is pushed to the middle of the volume and both sides of the substrate are covered with vapor. For $\varepsilon_{sf}>\varepsilon_d$, the liquid slab is attracted to one of the sides of the substrate and this remains so even

beyond $\varepsilon_{sf}=\varepsilon_w$ where it is more favorable that the liquid slab splits into two parts, both covering a side of the substrate with a vapor layer in between. Thus the partially wet state can be continued easily as a metastable state into the wet region (the reverse is also true for wet states in the partially wet region). These features can be recognized in Fig. 3 in which the $\partial\cos\theta/\partial\varepsilon_{sf}$ data are plotted as a function of ε_{sf}. Whereas the derivative reaches a plateau near the wetting point ε_w, it drops sharply to zero near ε_d. This means that the drying transition is continuous while the wetting transition is first order. A continuous drying transition is characterized by a behavior of $\cos\theta$ as

$$\cos\theta=-1+c(\varepsilon_{sf}-\varepsilon_d)^x, \quad \varepsilon_{sf}\geq\varepsilon_d \tag{3}$$

with c an arbitrary, positive constant. Renormalization calculations[16,17] predict $x=2/(1-\omega)$ with ω given by

$$\omega=\frac{k_BT}{4\pi\xi_v^2\gamma_{lv}} \tag{4}$$

with ξ_v the bulk correlation length of the vapor phase. It is difficult to estimate this length in such a dilute vapor phase as we encounter, but taking ξ_v to be larger than σ_{ff}, ω is smaller than $\omega=0.3$. Our data are not accurate enough to obtain a precise estimate of ω, which would also require a very precise knowledge of the drying point ε_d. They are, however, consistent with the bound on ω given above.

The consistency between the directly measured $\cos\theta$ and the measurements of its derivative can be seen in Fig. 2, which shows that the cosines can be reconstructed by integrating the $\partial\cos\theta/\partial\varepsilon_{sf}$ data with respect to ε_{sf}. As an aid to the numerical integration, a cubic spline was fitted to the $\partial\cos\theta/\partial\varepsilon_{sf}$ data, which fit was then integrated from the point $\cos\theta=-1$ at $\varepsilon_r=0.1$ onwards.

The points in Figs. 2 and 3 are obtained by decreasing ε_r. We also tested on the occurrence of hysteresis, which should not appear at a continuous transition, by increasing ε_{sf} from a completely dry system at $\varepsilon_f=0.10$ onwards. The two branches of $\partial\cos\omega/\partial\varepsilon_{sf}$ are shown in Fig. 4 zooming in on the drying transition. The branch of increasing ε_r (circles) remains a little longer in the completely dry state, resulting in a difference in $\partial\cos\theta/\partial\varepsilon_{sf}$ of the increasing and decreasing branch (crosses) at $\varepsilon_r=0.175$. The small differences at $\varepsilon_r=0.19$ and 0.22 seem not significant in view of the large fluctuations included in the averages. The fluctuations around the drying transition result primarily from small movements of the liquid slab. As the slab moves somewhat closer to the wall, the number of fluid particles in the first adsorbed layer increases significantly and $\partial\gamma_{sl}/\partial\varepsilon_{sf}$ drops while the opposite effect occurs when the slab moves a little bit further away from the wall. Compared with the fluctuations in the derivative of γ_{sl}, the derivative of γ_{sv} is virtually constant. We followed many of these systems until we had obtained 20 subaverages over 5200 time steps. We sometimes noticed correlations between three to five consecutive subaverages, indicating large scale fluctuations. The circles in Fig. 4 give values of $\partial\cos\theta/\partial\varepsilon_{sf}$ that point at an $\varepsilon_d\approx0.174$ whereas the crosses point at $\varepsilon_d=0.163$. The total surface free energy of the two branches does not differ significantly and therefore, we cannot decide which of the two branches is thermodynamically most stable. Thus, the occurrence of two branches can hardly be viewed as representing a hysteresis loop indicative of a first-order transition, but we

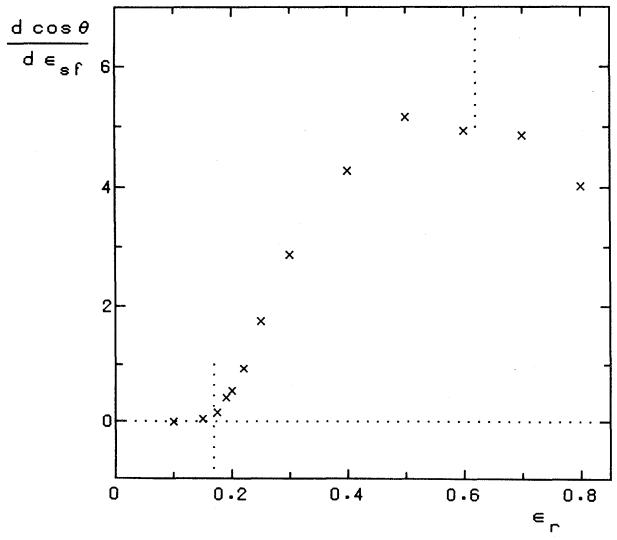

FIG. 3. The measured derivative of $\cos\theta$ with respect to ε_{sf} as a function of ε_r. The error bars are of the order of the symbol size. The vertical dotted lines denote the positions of the drying and wetting transition.

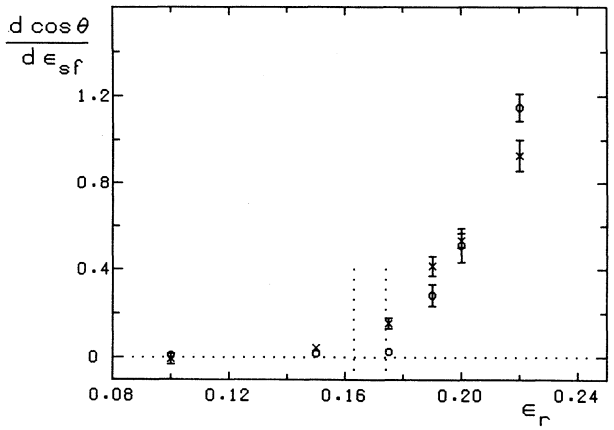

FIG. 4. The derivative of $\cos\theta$ with respect to ε_{sf} as a function of ε_r around the drying transition. The crosses are the same points as in the previous figure, they are obtained by decreasing ε_r. The circles are obtained by increasing ε_r from $\varepsilon_r=0.1$ onwards. If error bars are omitted, they are of the order of the symbol size. The two vertical dotted lines give the estimated bounds on the location of the drying transition.

attribute it to the large and persistent fluctuations around the phase transition. Contrary to Henderson and van Swol,[9] we see the large fluctuations as precursor effects of the continuous drying transition. Our best estimate is therefore $\varepsilon_d = 0.169 \pm 0.005$.

We must pay some attention to the center-of-mass motion, i.e., the "drift," that is generated in the system by the finite numerical accuracy of the molecular-dynamics calculation. As is customary in such simulations, the total momentum of the fluid is regularly set to zero (once every 5200 time steps in our case) to prevent the drift from getting a chance to become too large, and since almost all the fluid's mass is concentrated in the liquid slab, this most likely implies a slowing down of the slab's motion. Although we observed that the absence of any drift correction changes the motion of the liquid slab in systems around the drying transition, we could not detect a systematic feature in these differences.

So we conclude that, by an inspection of $\partial \cos\theta / \partial \varepsilon_{sf}$ instead of $\cos\theta$, we strongly improved the accuracy in the determination of both the order and location of the drying transition. Our simulations, treating large and rather realistic systems, show a surprising difference in character between the wetting and drying transition. Continuous drying transitions are also displayed by the density-functional calculations of both Velasco and Tarazona[11] and van Swol and Henderson.[7,9] In our simulations we see the structure smoothly change from a substrate-liquid to a substrate-vapor profile.

It is not yet clear where the differences with the results of Henderson and co-workers[9] originate from. Possible causes are the different representations of the wall or the much larger wall area in our simulations. The argument of Adams and Henderson that our simulations seriously underestimate the difference between the liquid and vapor bulk densities $n_l - n_v$ seems unlikely as we have encountered the bulk densities $n_l^* = 0.6640 \pm 0.006$ and $n_v^* = 0.0456 \pm 0.006$ in a series of simulations[12,14,18] and these values are consistent with recent simulations[19] of phase equilibria. We consider their objection that our computational box would be too small in the z direction to accommodate the type of fluctuations they observe, unlikely too. The continuous decrease of $\partial \cos\theta / \partial \varepsilon_{sf}$ already occurs in the range $0.25 < \varepsilon_f < 0.40$ when the liquid slab is still securely bound to the wall. The fluctuations in the slab's position very close to the drying transition seem not hindered by the presence of the wall opposite to the one at which the slab is adsorbed. Therefore, we have no indication that our geometry suppresses fluctuations that drive the liquid slab away from the wall and cause a discontinuous jump in $\partial \cos\theta / \partial \varepsilon_{sf}$ to $\partial \cos\theta / \partial \varepsilon_{sf} = 0$.

We are indebted to F. Lange and A. B. van Woerkom for assisting with the simulations. Part of this research was supported by the Stichting voor Fundamenteel Onderzoek der Materie (FOM), which is financially supported by the Nederlandse Organisatie voor Wetenschappelijk Onderzoek (NWO).

[1] For a review, see, e.g., S. Dietrich, in *Phase Transitions and Critical Phenomena,* edited by C. Domb and J. Lebowitz (Academic, London, 1988), Vol. 12.
[2] J. W. Cahn, J. Chem. Phys. **66**, 3667 (1977).
[3] C. Ebner and W. F. Saam, Phys. Rev. Lett. **38**, 1486 (1977).
[4] M. R. Moldover and J. W. Cahn, Science **207**, 1073 (1980).
[5] C. Ebner, Phys. Rev. A **23**, 1925 (1981).
[6] G. Langie and J. O. Indekeu, Phys. Rev. B **40**, 417 (1989).
[7] F. van Swol and J. R. Henderson, Phys. Rev. A **40**, 2567 (1989).
[8] E. Velasco and P. Tarazona, J. Chem. Phys. **91**, 7916 (1989).
[9] J. R. Henderson and F. van Swol, J. Phys. Condens. Matter. **2**, 4537 (1990); F. van Swol and J. R. Henderson, Phys. Rev. A **43**, 2932 (1991); P. Adams and J. R. Henderson (unpublished).
[10] F. van Swol and J. R. Henderson, Faraday Symp. Chem. Soc. **20**, 1 (1985).
[11] E. Velasco and P. Tarazona (private communication).
[12] J. H. Sikkenk, J. O. Indekeu, J. M. J. van Leeuwen, E. O. Vossnack, and A. F. Bakker, J. Stat. Phys. **52**, 23 (1988).
[13] M. J. P. Nijmeijer, C. Bruin, A. F. Bakker, and J. M. J. van Leeuwen, Physica A **160**, 166 (1989).
[14] M. J. P. Nijmeijer, C. Bruin, A. F. Bakker, and J. M. J. van Leeuwen, Phys. Rev. A **42**, 6052 (1990).
[15] A. F. Bakker and C. Bruin, in *Special Purpose Computers,* edited by B. J. Alder (Academic, London, 1988).
[16] E. Brézin, B. I. Halperin, and S. Leibler, J. Phys. (Paris) **44**, 775 (1983).
[17] D. S. Fisher and D. A. Huse, Phys. Rev. B **32**, 247 (1985).
[18] M. J. P. Nijmeijer, A. F. Bakker, C. Bruin, and J. H. Sikkenk, J. Chem. Phys. **89**, 3789 (1988).
[19] B. Smit, Ph.D. thesis, Rijksuniversiteit Utrecht, the Netherlands (1990).